Journal of Mathematical Chemistry Vol. 30, No. 1, July 2001 (© 2001)

On the mathematical properties of Distributed Approximating Functionals

Guowei Wei [a], Haixiang Wang [b], Donald J. Kouri [b,*], Manos Papadakis [c,**], Ioannis A. Kakadiaris [d] and David K. Hoffman [e,***]

[a] *Department of Computational Science, National University of Singapore, Singapore, 129260*
[b] *Department of Chemistry and Department of Physics, University of Houston, Houston, TX 77204-5641, USA*
[c] *Department of Mathematics, University of Houston, Houston, TX 77204-3476, USA*
[d] *Department of Computer Science, University of Houston, Houston, TX 77204-3475, USA*
[e] *Department of Chemistry and Ames Lab, Iowa State University, Ames, IA 50011, USA*

Received 10 September 2000; revised 8 May 2000

This work investigates some mathematical properties of the Distributed Approximating Functionals (DAFs). We prove that certain classes of DAFs yield Unity Approximations. Two distinct classes which serve as examples are the Hermite-DAFs and the Sinc-class DAFs. Detailed proofs are given. A wavelet generator is constructed using the Continuous Wavelet Transform with repect to the scale parameter. Taking the Gaussian function as the scaling function, a numerical experiment is carried out demonstrating the use of the resulting wavelet for edge detection.

KEY WORDS: Distributed Approximating Functionals (DAFs), wavelet generator, Gaussian function

1. Introduction

This paper is the first of a series of papers on the study of the mathematical properties of a certain class of functions, named Distributed A pproximating Functionals (DAFs) which were originally introduced by Hoffman, Kouri and coworkers [1–3]. The DAFs were first utilized as approximate Dirac delta kernels, in the sense that they were used to approximate, with respect to various norms, smooth functions, their various derivatives, and certain other linear transformations [4–6]. Discrete sampling of the action of the kernel on appropriate smooth functions was used to derive practical approximations. Some example applications of DAFs were for the numerical solution of certain ODEs and PDEs [4–6]. The empirical observation of controllable accuracy

* Research supported in part under National Science Foundation Grant CHE-0074311 and R.A. Welch Foundation Grant E-0608.
** Research supported by a New Faculty Research Award of the University of Houston.
*** The Ames Laboratory is operated for the Department of Energy by Iowa State University under Contract No. 2-7405-ENG82.

0259-9791/01/0700-0083$19.50/0

achieved in many such applications motivated Chandler and Gibson to analyze the convergence properties of the HDAFs [7]. Chandler and Gibson in [7] established a rigorous mathematical basis for what Hoffman, Kouri and coworkers were referring to as "delta sequences". They introduced the rigorous concept of unity approximations (see definition 3). In fact, both the HDAFs created by Hoffman, Kouri and coworkers and the "interpolating DAFs" created by Wei, Hoffman, Kouri and coworkers [4,8–10] yield unity approximations, as we prove in section 3. Moreover, in this section we generalize the class of Sinc DAFs. The practical significance of unity approximations is that functions belonging to certain "large" function spaces, and their derivatives, can be systematically approximated, with respect to the uniform norm, by sequences of functions produced by filtering the original function (see theorem 2). Essentially, this particular result establishes mathematically the character of DAFs as "delta sequences", as mentioned above.

More recently, DAFs were used with remarkable success as multiresolution scaling functions to generate wavelets for image processing applications [4,6,8–10]. The successful application of these ideas in a variety of domains suggests that there is a deep relation between DAFs and multiresolution techniques, both in univariate and multivariate settings. In section 2, we show that DAFs can be used for the detection of edges (singularities of functions) based on the Continuous Wavelet Transform (CWT), rather than the theory of multiresolution analysis (see theorem 1).

The first DAF developed, called the Hermit Distributed Approximating Functionals (HDAF), is not interpolative on the input grid points [1]. That is, the HDAF approximation to a suitable function at any grid point, x_j, is not exactly equal to the input data value. In contrast to the interpolative property, the HDAF approach to functional approximation has the property that there are no "special points". Another type of DAF, which we call Sinc-class DAFs, and two of its specific realizations, the *Sinc DAF* and *generalized de la Vallée Poussin* DAF, are discussed in detail in section 3.

We conclude this introduction with a few remarks to orient the reader. The space $\mathbf{L}^2(\mathbb{R})$ is the Hilbert space containing all measurable functions f defined on $\mathbb{R}$ with complex or real values such that $\int_{-\infty}^{+\infty} \| f(t)\|^2 \, \mathrm{d}t < +\infty$. This space possesses an inner product defined by

$$\langle f, g\rangle = \int_{-\infty}^{+\infty} f(t)\overline{g(t)} \, \mathrm{d}t. \tag{1}$$

The CWT on $\mathbf{L}^1(\mathbb{R})$ is defined in equation (6). Although an additional hypothesis, called the *admissibility condition*, must be imposed on the wavelet ψ to ensure the "exact reconstruction" of a wavelet-analyzed function, we will consider functions ϕ and ψ in $\mathbf{L}^1(\mathbb{R})$ suitable to define accurately the mappings σ and W given in section 2, without using the admissibility condition. Thus we will avoid giving the definition of a wavelet here. The hypotheses we impose on ϕ and ψ in section 2 are sufficient to ensure validity of theorem 1.

For $1 \leqslant p < +\infty$, we define the $\mathbf{L}^p(\mathbb{R})$ to be the linear spaces of measurable complex valued functions f such that $\int_{-\infty}^{+\infty} |f(t)|^p \, \mathrm{d}t < +\infty$. We define the norm $\| \cdot \|_p$

as

$$\|f\|_p := \left(\int_{-\infty}^{+\infty} \left|f(t)\right|^p \,\mathrm{d}t\right)^{1/p}. \tag{2}$$

Only for $p = 2$, $\mathbf{L}^p(\mathbb{R})$ is a Hilbert space. For all other cases, $\mathbf{L}^p(\mathbb{R})$ are Banach spaces (see [11] for more details). By $\|\cdot\|_\infty$ we denote the uniform norm on the space of bounded functions on $\mathbb{R}$.

Finally, a measurable function $F : [a, b] \to \mathbb{C}$ is absolutely continuous if there exists $f \in \mathbf{L}^1([a, b])$ such that

$$F(x) = \int_a^x f(t)\,\mathrm{d}t, \quad x \in [a, b]. \tag{3}$$

It is known that if F is absolutely continuous then it is continuous and differentiable almost everywhere (i.e., there exists a measurable subset A of $[a, b]$ such that $F'(t)$ exists for every $t \in [a, b]$). In fact, $F'(t) = f(t)$ almost everywhere in $[a, b]$. For absolutely continuous functions, integration by parts is true. The interested reader may refer to [11] for more details on absolute continuity.

2. Wavelet generation

2.1. Wavelet differentiation pairs

Holschneider [12] has given a very interesting perspective on the Continuous Wavelet Transform. Assume that ϕ is in $\mathbf{L}^1(\mathbb{R})$, bounded and uniformly continuous. Then for any arbitrary $f \in \mathbf{L}^1(\mathbb{R})$, $a > 0$, $b \in \mathbb{R}$ we define

$$\sigma_f(b, a) := \int_{-\infty}^{+\infty} \frac{1}{a}\overline{\phi\left(\frac{t-b}{a}\right)} f(t)\,\mathrm{d}t. \tag{4}$$

The integrability of f and ϕ implies that $\sigma_f(b, a)$ is well defined. In addition, the uniform continuity and the boundedness of ϕ imply that σ_f is a continuous function.

We can interpret the function σ_f as a continuous wavelet transform with respect to the window function ϕ. We will refer to ϕ as a *father wavelet*. We will consider the derivatives $\partial\sigma_f/\partial a$ in $(0, +\infty)$ and try to interpret them in terms of a continuous wavelet transform with respect to another window function. Thus, the idea is that $\partial\sigma_f/\partial a$ gives us the "rate" of the change of information from one scale to another.

In addition to the previous hypotheses, we assume that ϕ is differentiable and that $t\phi'(t)$ is bounded and absolutely integrable. Then

$$\psi(t) := \phi(t) + t\phi'(t) \tag{5}$$

is in $\mathbf{L}^1(\mathbb{R})$. We will refer to ψ as a *mother wavelet*. Next, we define

$$Wf(b, a) = \int_{-\infty}^{+\infty} \frac{1}{a}\overline{\psi\left(\frac{t-b}{a}\right)} f(t)\,\mathrm{d}t, \quad f \in \mathbf{L}^1(\mathbb{R}). \tag{6}$$

Theorem 1. If ϕ satisfies the preceeding hypotheses, then we have that

$$\frac{\partial \sigma_f}{\partial a} = -\frac{1}{a} W f. \tag{7}$$

Proof. Let $a \in \mathbb{R}^+$, $b \in \mathbb{R}$ and $\{h_n\}_n$ be an arbitrary sequence such that $\lim h_n = 0$. Without any loss of generality we can assume $|a + h_n| > a/2$ for every $n \in \mathbb{N}$. Let $|\phi(t)| \leqslant M_1$ and $|\phi'(t)| \leqslant M_2$, for every $t \in \mathbb{R}$. Then we have that

$$\frac{\sigma_f(b, a + h_n) - \sigma_f(b, a)}{h_n} = \int_{-\infty}^{+\infty} \frac{1}{h_n} \overline{\left[\frac{1}{a + h_n}\phi\left(\frac{t-b}{a+h_n}\right) - \frac{1}{a}\phi\left(\frac{t-b}{a}\right)\right]} f(t)\,\mathrm{d}t. \tag{8}$$

Let $t \in \mathbb{R}$; then we can consider $(1/a)\phi((t-b)/a)$ as a function of a. Since ϕ is differentiable, we can apply the Mean Value Theorem (considering a as a variable). Thus, for each h_n and t we obtain $\xi_{n,t} \in (a, a + h_n)$ such that

$$\begin{aligned} &\frac{1}{h_n}\left[\frac{1}{a + h_n}\phi\left(\frac{t-b}{a+h_n}\right) - \frac{1}{a}\phi\left(\frac{t-b}{a}\right)\right] \\ &\quad = -\frac{1}{(a+\xi_{n,t})^2}\phi\left(\frac{t-b}{a+\xi_{n,t}}\right) - \frac{t-b}{(a+\xi_{n,t})^3}\phi'\left(\frac{t-b}{a+\xi_{n,t}}\right). \end{aligned}$$

Considering the right-hand side of the previous equation as a function of t we note the following. First, the term $(a+\xi_{n,t})^{-2}$ is absolutely bounded by $4/a^2$ for every n because $\xi_{n,t} \in (a, a+h_n)$ and $|a + h_n| > a/2$ for every n; second, for every n the function

$$\frac{t-b}{a+\xi_{n,t}}\phi'\left(\frac{t-b}{a+\xi_{n,t}}\right)$$

is absolutely bounded by M_2. Therefore, we have that for every t and n

$$\left|\frac{1}{(a+\xi_{n,t})^2}\phi\left(\frac{t-b}{a+\xi_{n,t}}\right) + \frac{t-b}{(a+\xi_{n,t})^3}\phi'\left(\frac{t-b}{a+\xi_{n,t}}\right)\right| \leqslant \frac{4}{a^2}(M_1 + M_2).$$

Since f is in $\mathbf{L}^1(\mathbb{R})$, we have that for every n the integrand in the right-hand side of equation (8) is dominated by the function $(4/a^2)(M_1 + M_2) f$. On the other hand,

$$\lim_{n\to\infty} \frac{1}{h_n}\overline{\left[\frac{1}{a + h_n}\phi\left(\frac{t-b}{a+h_n}\right) - \frac{1}{a}\phi\left(\frac{t-b}{a}\right)\right]} f(t) = -\frac{1}{a^2}\overline{\psi_a(t-b)}\, f(t).$$

The latter limit follows immediately from the definition of ψ and a trivial calculation of $\partial\phi_a(t)/\partial a$. Now using Lebesgue's Dominated Convergence theorem [13, theorem 12.30] we obtain that

$$\frac{\partial \sigma_f}{\partial a}(b, a) = -\frac{1}{a}\int_{-\infty}^{+\infty} \frac{1}{a}\overline{\psi\left(\frac{t-b}{a}\right)} f(t)\,\mathrm{d}t.$$

This completes the proof of theorem 1. □

Moreover, if ψ shares the same properties with ϕ, then the second-order derivative $\partial^2\sigma_f/\partial a^2$ can be obtained as follows:

$$\begin{aligned}\frac{\partial^2\sigma_f}{\partial a^2} &= \frac{\partial}{\partial a}\left(-\frac{1}{a}Wf\right)\\ &= \frac{1}{a^2}Wf - \frac{1}{a}\frac{\partial Wf}{\partial a}\\ &= \frac{1}{a^2}(Wf + W_1 f),\end{aligned}$$

where

$$W_1 f(b,a) = \int_{-\infty}^{+\infty} \frac{1}{a}\overline{\psi_1\left(\frac{t-b}{a}\right)} f(t)\,\mathrm{d}t \quad \text{and} \quad \psi_1 = \big(t\psi(t)\big)'.$$

In addition to the previous assumptions on ϕ and ψ, now assume that ψ is in $\mathbf{L}^1(\mathbb{R})$ and $\lim_{t\to\pm\infty}|t\phi(t)| = 0$. Notice that

$$\frac{\mathrm{d}}{\mathrm{dt}}\big(t\phi(t)\big) = \phi(t) + t\phi'(t).$$

Therefore, $t\phi(t)$ is absolutely continuous, and for every $\rho > 0$,

$$\rho\phi(\rho) + \rho\phi(-\rho) = \int_{-\rho}^{+\rho} \psi(t)\,\mathrm{d}t. \tag{9}$$

But $\lim_{t\to\pm\infty}|\phi(t)| = 0$ implies that $\lim_{\rho\to\pm\infty}|\rho\phi(\rho) + \rho\phi(-\rho)| = 0$. Thus,

$$\int_{-\infty}^{+\infty} \psi(t)\,\mathrm{d}t = 0. \tag{10}$$

This property is a necessary condition for mother wavelets (essentially it is the condition that ψ has a vanishing “DC”-component).

We would like to conclude the discussion on theorem 1 with a comment on the properties of the father and mother wavelets. The hypothesis that both wavelets are absolutely integrable has not been used in the proof of theorem 1. We added this particular hypothesis because it is customary to define wavelet transforms so that they are absolutely or square integrable functions.

Let us now see how Distributed Approximating Functionals produce pairs $\{\phi, \psi\}$ satisfying the previous hypotheses. Let $\phi \in C^n(\mathbb{R})$. Define the differential operator $G^{(m)}$ by the following:

$$G^{(0)} = xI, \tag{11}$$

$$G^{(n)} = x\frac{\partial^n}{\partial x^n} + n\frac{\partial^{n-1}}{\partial x^{n-1}}, \tag{12}$$

where $n = 1, 2, 3, \dots, m$. Now set

$$\psi_n = G^{(n)}\phi, \tag{13}$$

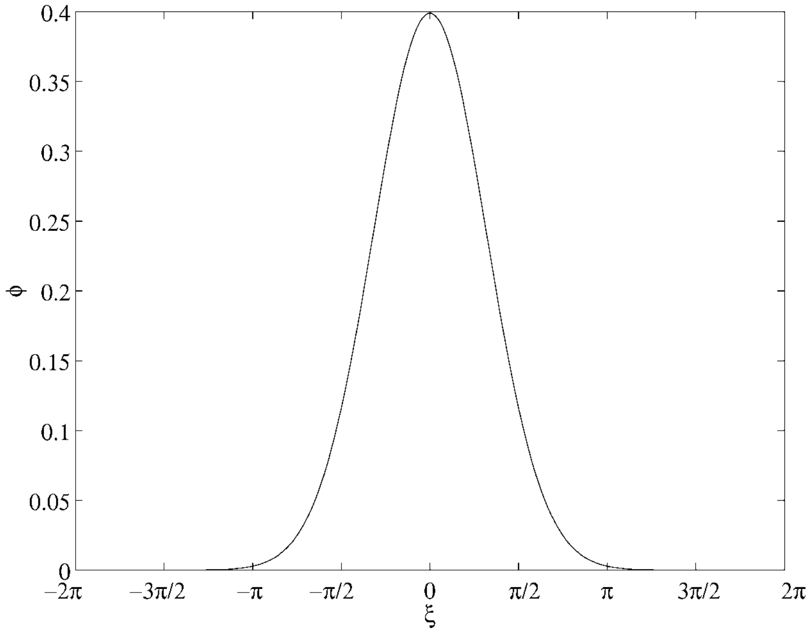

Figure 1. Plot of function ϕ_a with $a = 1.0$.

where $\phi \in C^m$ and $n = 0, 1, 2, \ldots, m$.

In the following, we present some examples to illustrate these ideas.

Example 1 (Mexican hat wavelets based on the Gaussian function as the father wavelet). We take the following function:

$$\phi(x) = \frac{1}{\sqrt{2\pi}} \mathrm{e}^{-x^2/2} \tag{14}$$

as our father wavelet (see figure 1), and for $n = 1$, equation (13) gives (see figure 2):

$$\psi_1(x) = \frac{1}{\sqrt{2\pi}} \bigl(1 - x^2\bigr) \mathrm{e}^{-x^2/2}. \tag{15}$$

The function ψ_1 is the well-known Mexican hat wavelet [14]. For $n = 2$ and $n = 3$, we get (see figures 3 and 4, respectively)

$$\psi_2(x) = \frac{1}{\sqrt{2\pi}} \bigl(x^3 - 3x\bigr) \mathrm{e}^{-x^2/2}, \tag{16}$$

and

$$\psi_3(x) = \frac{1}{\sqrt{2\pi}} \bigl(- x^4 + 6x^2 - 3\bigr) \mathrm{e}^{-x^2/2}. \tag{17}$$

The result for $n = 3$ is an interesting “Mexican superhat wavelet”.

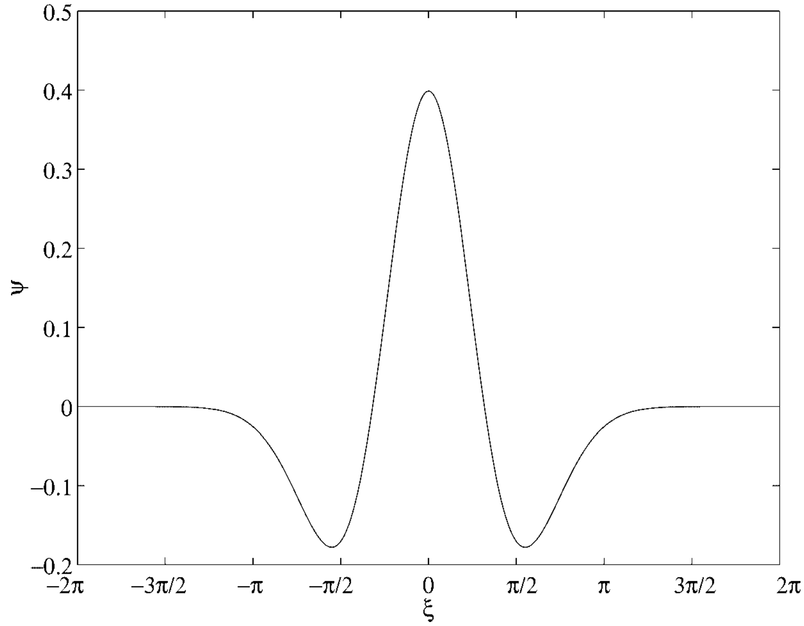

Figure 2. Plot of function $\psi_{a,1}$ with $a = 1.0$.

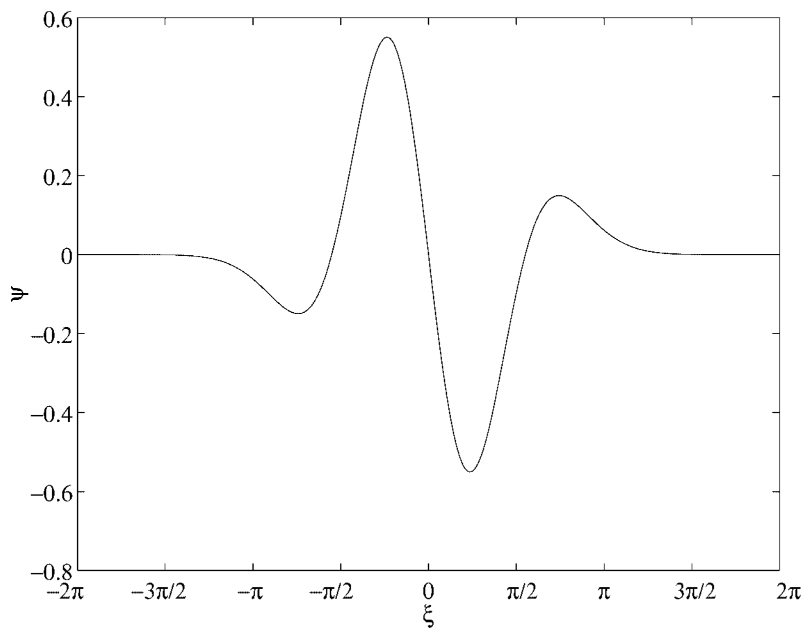

Figure 3. Plot of function $\psi_{a,2}$ with $a = 1.0$.

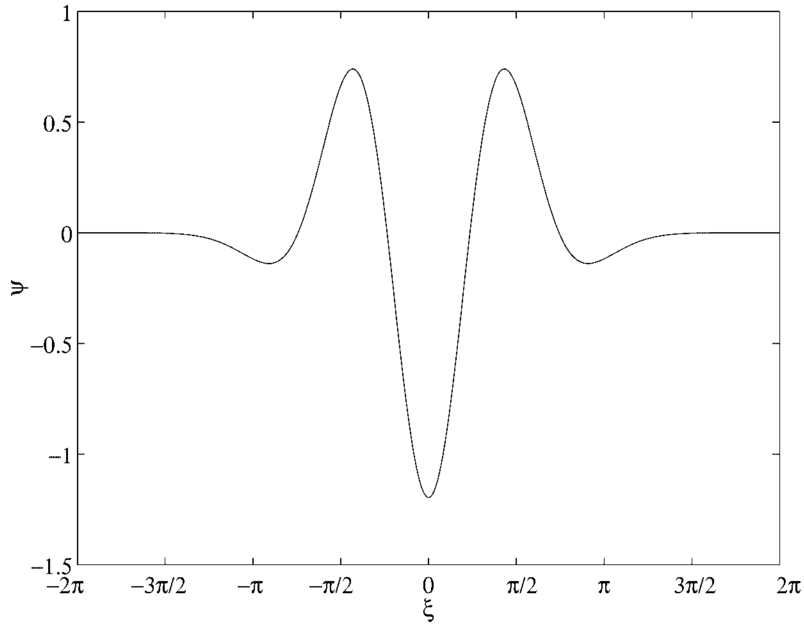

Figure 4. Plot of function $\psi_{a,3}$ with $a = 1.0$.

If one instead chooses the Sinc-DAF [8]

$$\phi(x) = \frac{1}{\sqrt{2\pi}} \mathrm{e}^{-x^2/2} \frac{\sin(\pi x)}{\pi x}$$

(see figure 5) as the father wavelet, and sets $n = 1$, equation (13) gives (see figure 6)

$$\psi_1 = \frac{1}{\sqrt{2\pi}} \mathrm{e}^{-x^2/2} \left[\cos(\pi x) - \frac{\sin(\pi x)}{\pi} x \right]. \tag{18}$$

For $n = 2$, we obtain (see figure 7)

$$\psi_2 = \frac{1}{\sqrt{2\pi}} \mathrm{e}^{-x^2/2} \left[\sin(\pi x)\left(x^2 - 1 - \pi^2\right) - \cos(\pi x) 2\pi x \right]. \tag{19}$$

Theorem 1 establishes that our continuous wavelet transform can be utilized for the calculation of the first derivative of another Continuous Wavelet Transform with respect to the scale. Every function in $\mathbf{L}^2(\mathbb{R})$ admits a representation with respect to the CWT. This representation maps $\mathbf{L}^2(\mathbb{R})$ isometrically onto $\mathbf{L}^2(\mathbb{R}^2)$ with an appropriate measure, where the first coordinate represents the time or the spatial domain and the second the scale. In the CWT the frequency domain is divided into intervals of the form $[-2^{p-1}, -2^p) \cup [2^p, 2^{p+1})$ and we refer to p as the scale. More specifically, we do not directly consider frequencies but we replace them with the scale.

Nevertheless, there is a reciprocity between the scale and the frequency; the high frequency content is captured within higher scales and the low frequency within the lower scales. The higher scale analysis thus includes more information about the finer

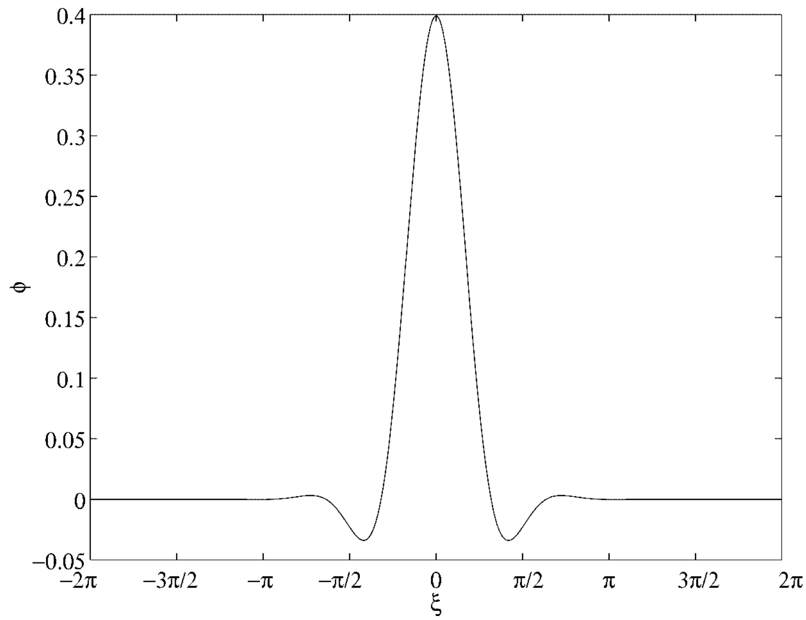

Figure 5. Plot of function ϕ_a with $a = 1.0$.

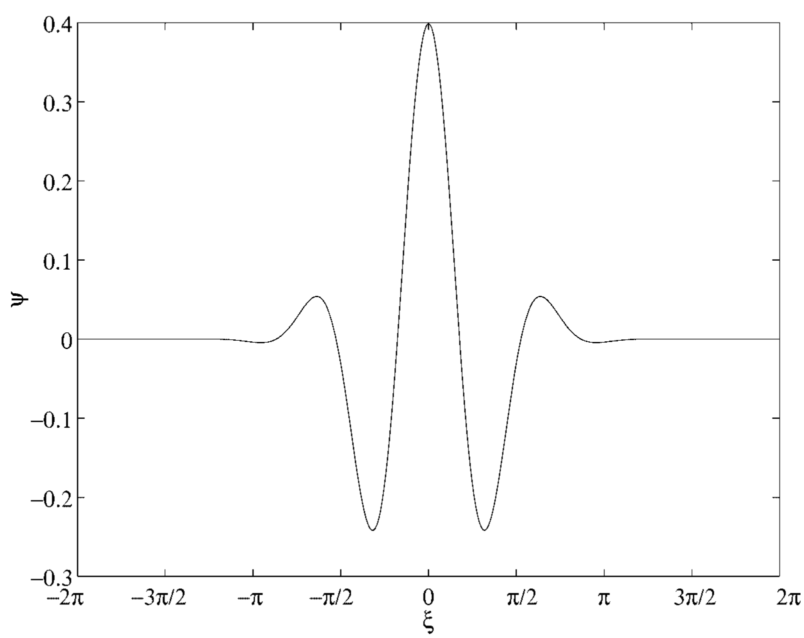

Figure 6. Plot of function $\psi_{a,1}$ with $a = 1.0$.

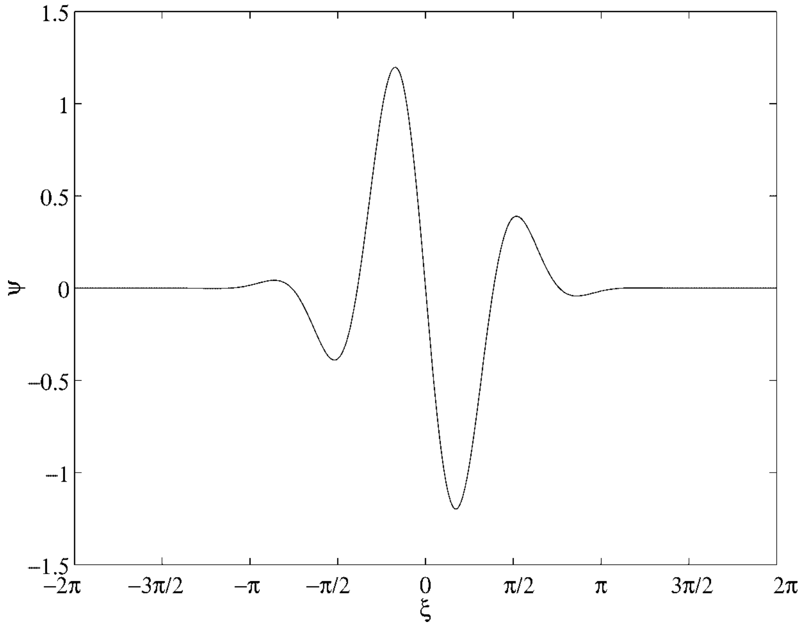

Figure 7. Plot of function $\psi_{a,2}$ with $a = 1.0$.

details of the signal, while lower scale analysis gives the average characteristics or a "blurred" version of the signal. All these intuitive comments, which are well known in the wavelet community simply reflect that differentiating the CWT of a function with respect to scale gives us locally the rate of the change of the details of a signal.

In regions of rapid variation, partial derivatives of the CWT of a given signal with respect to scale take on values whose moduli are significantly greater than zero, at least for certain ranges of scale. Thus, such derivatives can assist us in identifying the regions where the signal is rapidly changing. Edges are regions where the smoothness of the luminosity function of an image changes much faster than in neighboring regions. Therefore, theorem 1 and the preceding discussion suggest that the CWT with respect to the mother wavelet ψ (as defined in theorem 1) provides us a tool to detect edges in an image.

Below we present the results of some illustrative experiments in edge detection using the DAF-based CWT. We consider two test functions (whose graphs are shown in figures 8 and 13) that were selected because they represent typical models for edges. Figures 11 and 16 respectively show the results of the CWT of these functions with respect to the father wavelet ϕ given by equation (14). Notice that as the scale increases, we obtain more and more accurate approximations to the original functions. For the function shown in figure 8, it is very clear that discontinuities occur at $t = 200$ and $t = 300$ in the time domain (see figure 11). The CWT of this function for coarser scales smoothes these two discontinuities. If we consider carefully the behavior of the CWT in figure 11 at $t = 200$ and $t = 300$ we see that over the scale interval $a = 0.04$ to 0.13

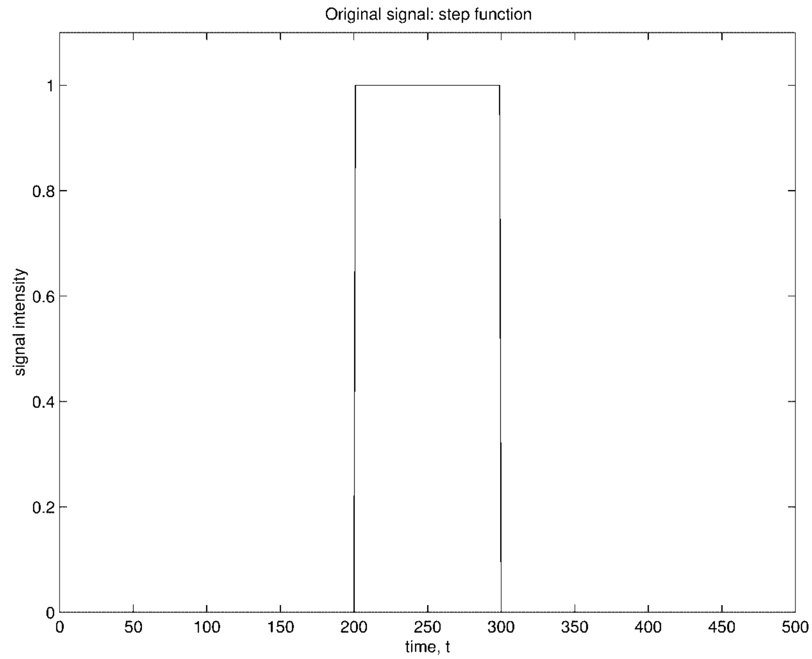

Figure 8. Plot of the original signal: a step function with discontinuities at $t = 200$ and $t = 300$.

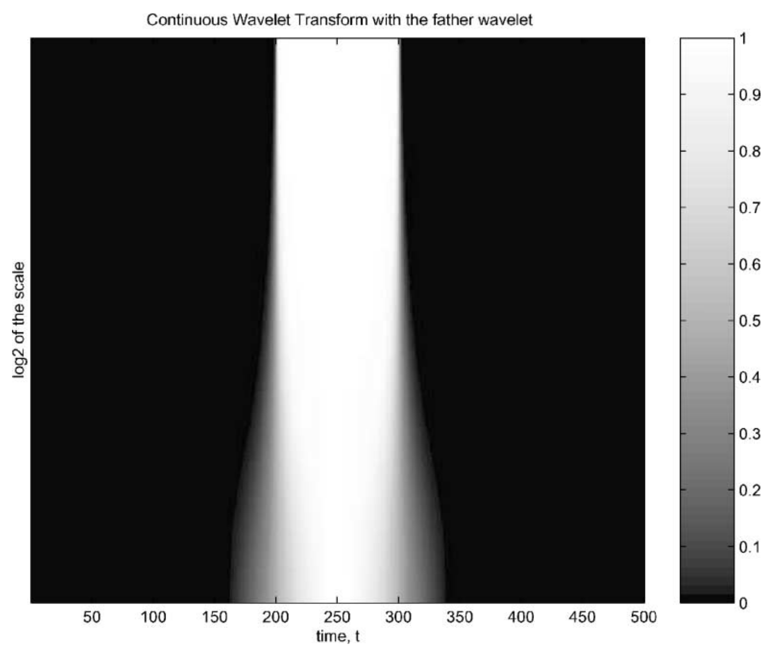

Figure 9. Graph of the Continuous Wavelet Transform of our step function with the father wavelet versus the natural log of the scales, the upper part is the finer scale. This type of graph of the CWT is often refered to as scalogram.

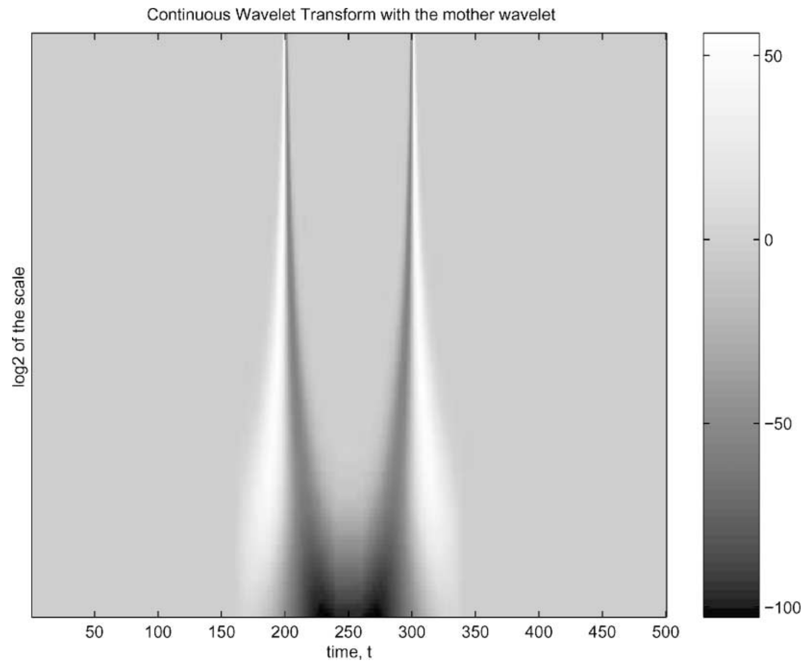

Figure 10. Scalogram of the step function in figure 8 with respect to the mother wavelet.

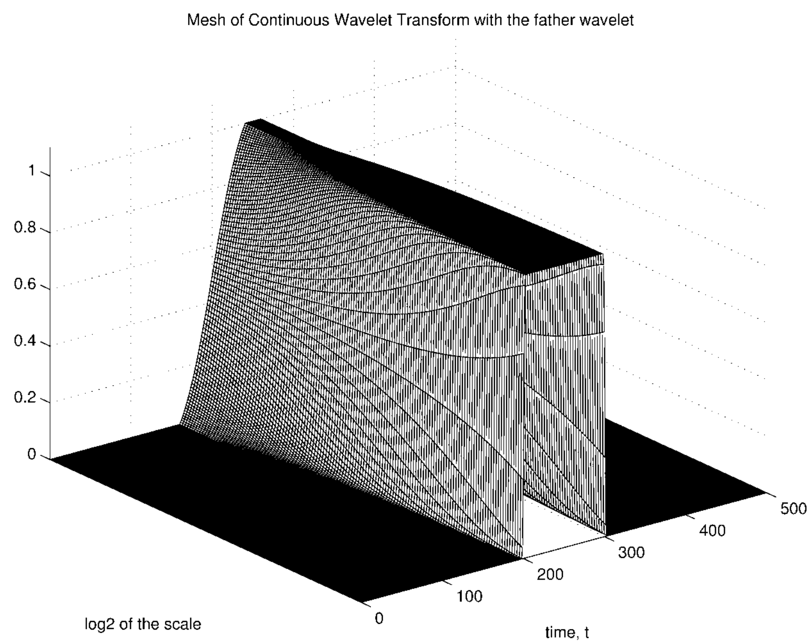

Figure 11. Mesh of the Continuous Wavelet Transform depicted in figure 9.

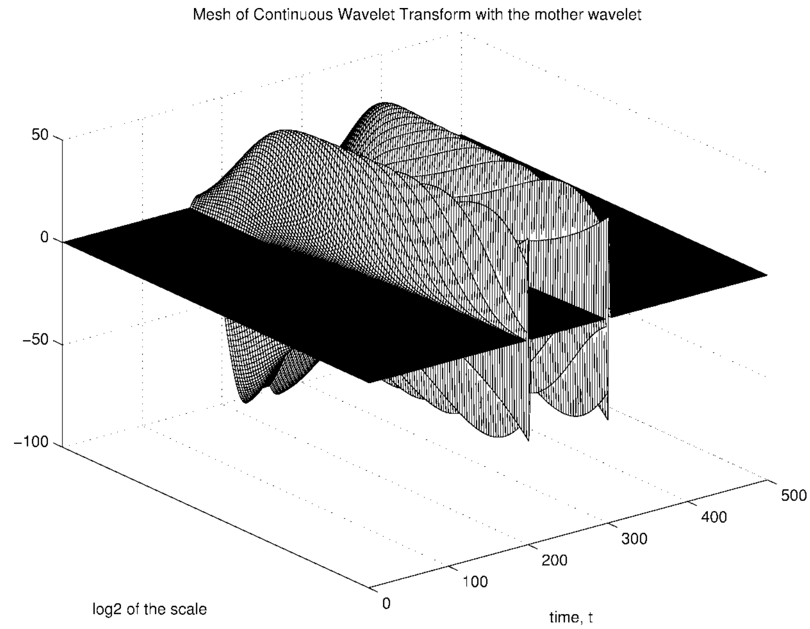

Figure 12. Mesh of the Continuous Wavelet Transform depicted in figure 10.

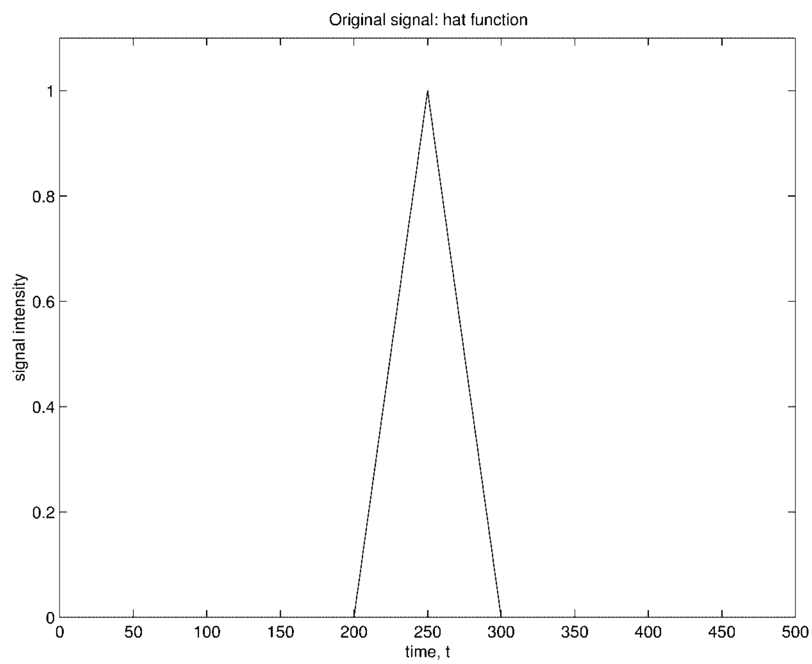

Figure 13. Plot of the original signal: a hat function with discontinuities at $t = 200$, $t = 300$ and $t = 250$.

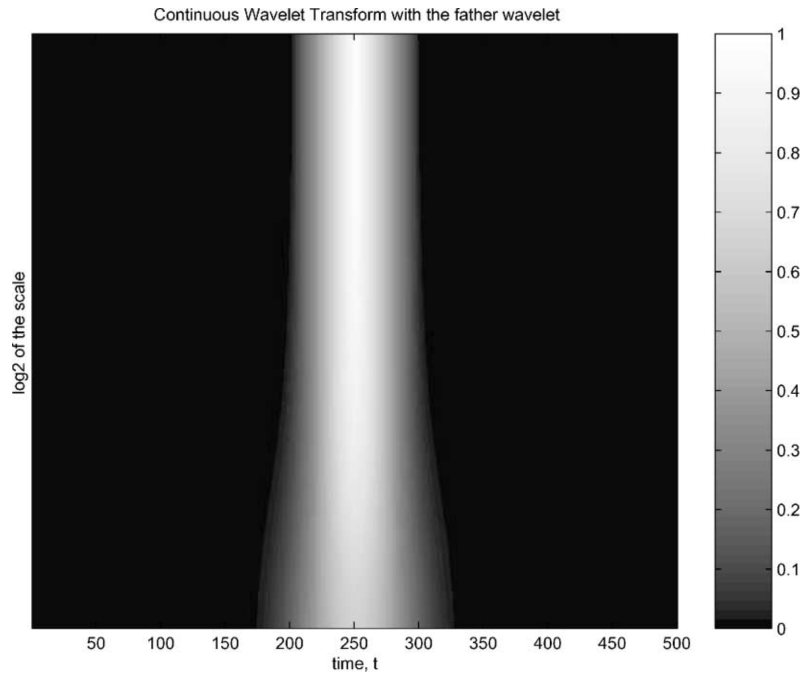

Figure 14. Scalogram of the hat function in figure 13 with respect to the father wavelet.

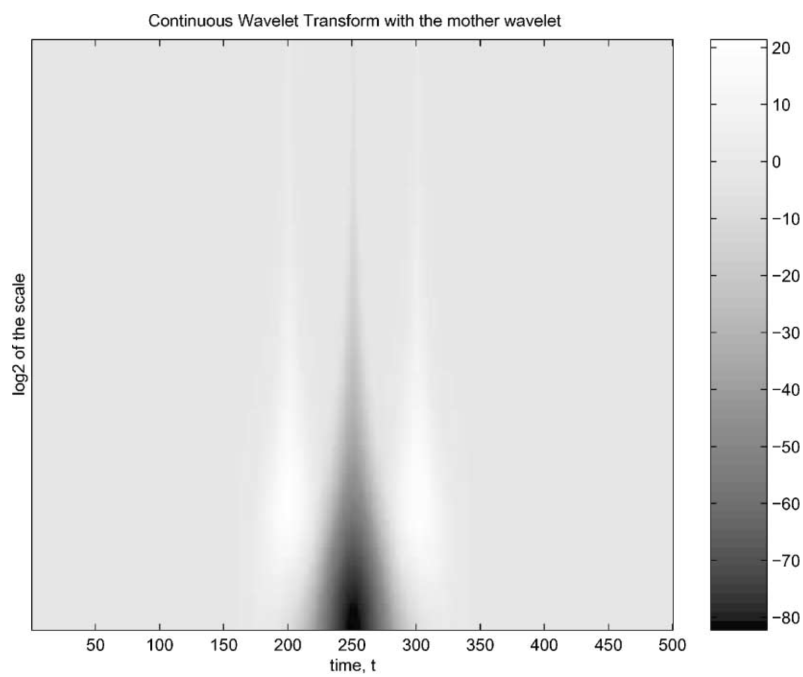

Figure 15. Scalogram of the hat function in figure 13 with respect to the mother wavelet.

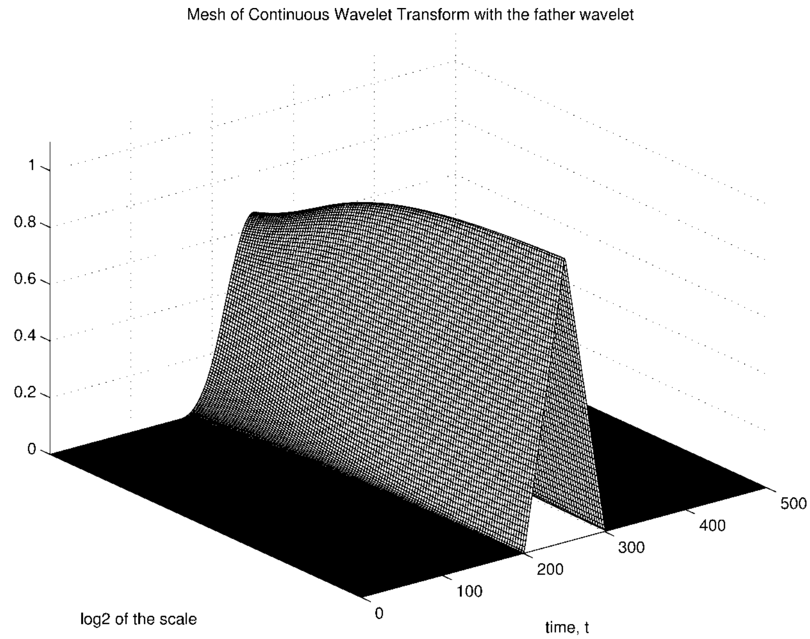

Figure 16. Mesh of the Continuous Wavelet Transform depicted in figure 14.

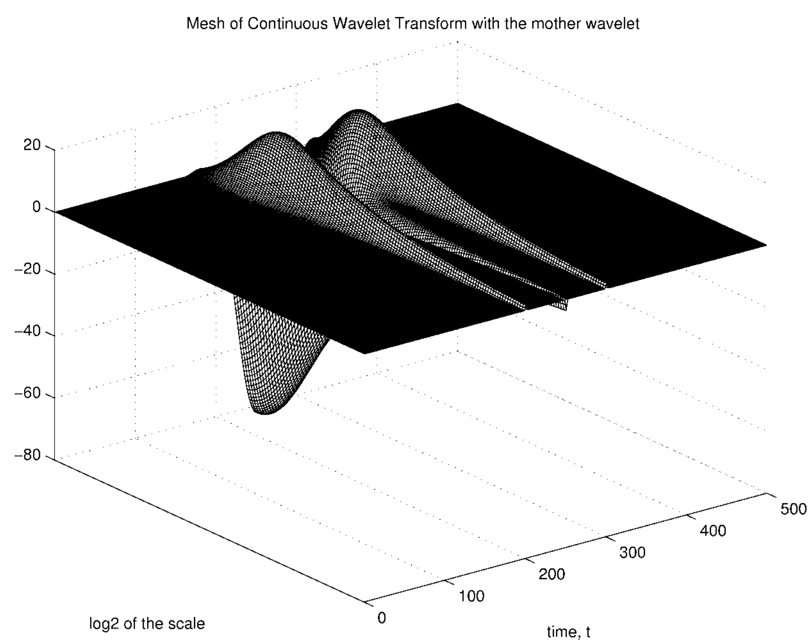

Figure 17. Mesh of the Continuous Wavelet Transform depicted in figure 15.

there is no significant change in the value of the CWT of the function f (see figure 8), but for scales from a equal to 0.13 up to 1.5, large changes are observed. Figure 10 shows the scalogram, i.e., the values of the CWT, of the function in figure 8 with respect to the mother wavelet ψ (corresponding to the particular father wavelet ϕ, with respect to which the CWT in figure 11 was calculated). Recall that the CWT of the function with the mother wavelet ψ is the first-order partial derivative, which respect to the scale, of the CWT of the function with the father wavelet. Carefully examining the values of the scalogram in figure 10 at $t = 200$ and $t = 300$ we see that at high scales, there is a rapid increase followed immediately by a rapid decrease, with values approximately zero away from the discontinuities. At lower scale values, one finds a smoothing of the discontinuity. It is clear that the rapidly changing values of the scalogram of figure 10, concentrated at $t = 200$ and $t = 300$, for higher scales indicate an extreme sensitivity of this method for the detection of edges.

In figure 13 the hat function is continuous but not C^1. Notice that the scalogram in figure 15 identifies the points $t = 200$, $t = 300$ and $t = 250$ as "edges", where the first-order partial derivative of the input signal does not exist. Experiments with different examples of father and mother wavelets, e.g., those associated with Hermite and Sinc DAFs, show similar behavior.

The present results are very encouraging. However, further experimentation with 2-D images is needed, along with additional in-depth analysis of the mathematics. This is part of an ongoing project dealing with the development of the mathematical theory of DAFs.

3. Distributed approximating functionals and unity approximations

In this section, we shall discuss some rigorous mathematical properties of DAFs, especially in connection with two classes of DAFs.

Definition 1. A function $f:\mathbb{R} \to \mathbb{R}$ is said to be in the Schwartz class if it is C^∞ and satisfies the property: for every $n = 0, 1, 2, \dots,$

$$\sup\left\{|x|^k \left|f^{(n)}(x)\right|:\ x \in \mathbb{R}\right\} < +\infty, \tag{20}$$

where $f^{(n)}$ is the nth derivative of f.

The set of all functions in the Schwartz class is denoted by $S(\mathbb{R})$ and is a locally convex topological vector space.

Recently, Chandler and Gibson studied some of the mathematical properties of the DAFs [7]. Among other things they introduce an interesting general definition of "unity approximations", to which DAFs belong, and whose essentials we review below.

Definition 2 [7]. Let M be a non-negative integer, let S_M be the set of measurable functions $\hat{f}: \mathbb{R} \to \mathbb{C}$ such that

$$\|\hat{f}\|_M := \int_{-\infty}^{+\infty} |\hat{f}(\xi)| w_M(\xi)\, \mathrm{d}\xi < +\infty, \tag{21}$$

where $w_M(\xi) := \sum_{m=0}^{M} |\xi|^m$.

It can be proved that S_M is a Banach space with respect to $\|\cdot\|_M$, i.e., $\|\cdot\|_M$ is a norm and with respect to this norm, Cauchy sequences of functions in S_M converge in S_M. For details, the reader should refer to [7].

Next, we will follow the formalism of [7] but slightly modified. Let $\mathcal{F}$ be the Fourier transform in $\mathbf{L}^1(\mathbb{R})$. For $f \in \mathbf{L}^1(\mathbb{R})$ and $\xi \in \mathbb{R}$ we define

$$\mathcal{F}(f)(\xi) = \hat{f}(\xi) := \frac{1}{\sqrt{2\pi}} \int_{-\infty}^{+\infty} f(x) \mathrm{e}^{-\mathrm{i}x\xi}\, \mathrm{d}x. \tag{22}$$

Plancherel's theorem establishes that $\mathcal{F}$ defined on $\mathbf{L}^1(\mathbb{R}) \cap \mathbf{L}^2(\mathbb{R})$ can be extended to a unitary operator defined on the whole $\mathbf{L}^2(\mathbb{R})$ (with values in $\mathbf{L}^2(\mathbb{R})$). For notational convenience, we will assume that $\mathcal{F}$ defined by equation (22) is always defined on $\mathbf{L}^2(\mathbb{R})$, but if $f \in \mathbf{L}^1(\mathbb{R}) \cap \mathbf{L}^2(\mathbb{R})$, then we can and will properly use the above equation.

Lemma 1 [7]. The following are true:

(a) $S(\mathbb{R})$ is contained in S_M, for every $M \geqslant 0$;

(b) S_M is a subspace of $\mathbf{L}^1(\mathbb{R})$, and $\|\cdot\|_1 \leqslant \|\cdot\|_M$.

Statement (b) of the above lemma shows that it is legitimate to define the Fourier transform for every $f \in S_M$. So we define $\mathcal{F}_M := \mathcal{F}(S_M) \cap \mathbf{L}^1(\mathbb{R})$. By the general properties of the Fourier transform every element of $\mathcal{F}_M$ is a uniformly continuous bounded function. Since $\mathcal{F}(S(\mathbb{R})) \subseteq S(\mathbb{R})$, the statement (a) of lemma 1 shows that $S(\mathbb{R})$ is contained in $\mathcal{F}_M$. This implies the following corollary.

Corollary 1 [7]. $\mathcal{F}_M \cap \mathbf{L}^P(\mathbb{R})$ is dense in every $\mathbf{L}^p(\mathbb{R})$ for $1 \leqslant p < \infty$.

Recall that if f is bounded then $\|\cdot\|_\infty := \sup\{|f(x)|: x \in \mathbb{R}\}$, and that $\|\cdot\|_\infty$ is a norm for the space of bounded functions defined on $\mathbb{R}$. Assume that $M \geqslant 1$. The definition of $\mathcal{F}_M$ does not provide a criterion to determine easily whether a uniformly continuous, absolutely integrable, bounded function defined on $\mathbb{R}$ belongs to $\mathcal{F}_M$ or not. Suppose that f is such a function and that we want to check whether f is in $\mathcal{F}_M$ or not. If f is in $\mathcal{F}_M$, then there exists $g \in S_M$ such that $f = \hat{g}$,

$$\hat{f}(\xi) := \frac{1}{\sqrt{2\pi}} \int_{-\infty}^{+\infty} f(x) \mathrm{e}^{-\mathrm{i}x\xi}\, \mathrm{d}x = \frac{1}{\sqrt{2\pi}} \int_{-\infty}^{+\infty} \hat{g}(x) \mathrm{e}^{-\mathrm{i}x\xi}\, \mathrm{d}x. \tag{23}$$

By the invertibility properties of the Fourier transform we conclude that $\hat{f}(\xi) = g(-\xi)$ almost everywhere[1] $\xi \in \mathbb{R}$, so $\hat{f}(-\xi) = g(\xi)$. Therefore, if $f \in \mathcal{F}_M \cap \mathbf{L}^1(\mathbb{R})$ then $\hat{f}(-\cdot) \in S_M$. Assuming that $f \in \mathbf{L}^1(\mathbb{R})$ is uniformly continuous, and $\hat{f}(-\cdot) \in S_M$, then for $x \in \mathbb{R}$ we have that

$$\mathcal{F}\big(\hat{f}(-\cdot)\big)(x) = \frac{1}{\sqrt{2\pi}} \int_{-\infty}^{+\infty} \hat{f}(\xi) \mathrm{e}^{\mathrm{i}x\xi}\, \mathrm{d}\xi = f(x), \tag{24}$$

since f is continuous at every $x \in \mathbb{R}$ and $\hat{f} \in \mathbf{L}^1(\mathbb{R})$.

Thus, $f \in \mathcal{F}_M$. Therefore, we conclude the following convenient characterization of the space $\mathcal{F}_M$, if $M \geqslant 1$.

Proposition 1. Let $M \geqslant 1$, $f \in \mathbf{L}^1(\mathbb{R})$ be a bounded uniformly continuous function. Then $f \in \mathcal{F}_M$ if and only if $\hat{f}(-\cdot) \in S_M$.

For the case $M = 0$, we have that $\mathcal{F}_M = A(\mathbb{R})$, the Banach space of the Fourier transforms of the absolutely integrable functions.

Definition 3 [7]. A sequence $\{\chi_n\}_{n\in\mathbb{N}}$ of unity approximations is a sequence of uniformly continuous elements of $\mathcal{F}_1$, satisfying the following properties: there exists $C > 0$ such that

(a) $\|\hat{\chi}_n\|_\infty \leqslant C$ for every $n \in \mathbb{N}$;

(b) for almost every $\xi \in \mathbb{R}$, $\lim_{n\to\infty} \hat{\chi}_n(\xi) = 1$.

The sequences of unity approximations are generalizations of the delta sequences introduced in the series of papers by Hoffman, Kouri and their collaborators [1–6,8–10]. Finally, the main result due to Chandler and Gibson [7] is the following:

Theorem 2 [7]. Let $\{\chi_n\}_{n\in\mathbb{N}}$ be a sequence of unity approximations. Let $M \geqslant 0$ and $f \in \mathcal{F}_M$. The following are true:

(a) the operator $C_n : \mathcal{F}_M \to \mathcal{F}_M$ defined by $C_n f := \mathcal{F}(\hat{\chi}_n \hat{f})$, where $f \in \mathcal{F}_M$, is a well-defined, bounded operator;

(b) for every $m = 0, 1, 2, \ldots, M$ and $n \in \mathbb{N}$, $f^{(m)}$, $(C_n f)^{(m)}$ belongs to $\mathcal{F}_M$;

(c) $\lim_{n\to\infty} \|f^{(m)} - (C_n f)^{(m)}\|_\infty = 0$ for every $m = 0, 1, 2, \ldots, M$.

The operators C_n are called *Continuous DAF operators*. Notice that by the definition of $\mathcal{F}_M$ and the general properties of the Fourier transform, if $f \in \mathcal{F}_M$ then $f \in C^M$.

Also it is not hard to see (but we will omit the details of the proof here) that

$$(C_n f)(x) = \int_{-\infty}^{+\infty} \chi_n(x - y) f(y)\, \mathrm{d}y, \tag{25}$$

where $\chi_n := \mathcal{F}(\hat{\chi}_n(-\cdot))$.

[1] Such $a - \xi$ is a Lebesgue point for g (see [15]).

Remark 1. Theorem 2 shows that $\{\hat{\chi}_n\}_{n\in\mathbb{N}}$ can be considered as a sequence of low band-pass filters. If we consider $\{\chi_n\}_{n\in\mathbb{N}}$, then the latter sequences yield sequences of functions that are similar to approximate identities in the time-domain, as equation (25) indicates in particular. Moreover, theorem 2 shows that for $\mathcal{F}_M$ which eventually contains all "nice" functions, unity approximations give *uniform approximations* of all functions in $\mathcal{F}_M$ and of their derivatives up to order M. But the fact that $\{\chi_n\}_{n\in\mathbb{N}}$ and in particular DAF functions can be considered as band-pass filters indicates that DAFs can be used as scaling functions for multiresolution analysis in $\mathbf{L}^2(\mathbb{R})$ and more generally in $\mathbf{L}^2(\mathbb{R}^n)$. This particular property of DAF functions is currently under investigation.

The latter equation establishes that $\{\chi_n\}_n$ is a "delta sequence".

We will now discuss several classes of DAF functions and prove explicitly that they yield unity approximations $\{\phi_n\}_{n=1}^{\infty}$ of the type defined by Chandler and Gibson [7]. Therefore, for every such sequence $\{\phi_n\}_{n=1}^{\infty}$ of DAF functions, we must establish that the following three properties are true.

1. Every $\phi_n \in \mathbf{L}^1(\mathbb{R}) \cap \mathcal{F}_1$ belongs to S_1, or equivalently,

$$\int_{-\infty}^{+\infty} \big(1 + |\xi|\big)\big|\hat{\phi}_n(\xi)\big| \,\mathrm{d}\xi < +\infty,$$

   and it is uniformly continuous.

2. $\|\hat{\phi}_n(\xi)\|_\infty \leqslant C$ for every $n \in \mathbb{N}$ and $\xi \in \mathbb{R}$ for some positive constant C.

3. For almost every $\xi \in \mathbb{R}$, $\lim_{n\to\infty} \hat{\phi}_n(\xi) = 1$.

The uniform continuity of the classes of sequences of DAF functions which we study in sections 3.1 and 3.2 is apparent from their definition.

3.1. *Hermite DAFs*

Hermite DAFs ϕ_N $(N \geqslant 1)$ are given by the following formula:

$$\phi_{N,\sigma}(x) := \frac{1}{\sqrt{2\pi}\sigma} \mathrm{e}^{-x^2/(2\sigma^2)} \sum_{n=0}^{N} \left(\frac{1}{4}\right)^n \frac{1}{n!} H_{2n}\left(\frac{x}{\sqrt{2}\sigma}\right), \tag{26}$$

where the function H_{2n} is the even-order Hermite polynomial. The Fourier transform of the Hermite DAF is given by

$$\hat{\phi}_{N,\sigma}(\xi) = \mathrm{e}^{-\xi^2\sigma^2/2} \sum_{n=0}^{N} \frac{(\xi^2\sigma^2)^n}{2^n n!}. \tag{27}$$

Then for $M \geqslant 1$ we have that

$$\int_{-\infty}^{+\infty} \left(1 + |\xi| + |\xi|^2 + \cdots + |\xi|^M\right) \left|\hat{\phi}_{N,\sigma}(\xi)\right| \mathrm{d}\xi$$
$$= \int_{-\infty}^{+\infty} \left(1 + |\xi| + |\xi|^2 + \cdots + |\xi|^M\right) \mathrm{e}^{-\xi^2\sigma^2/2} \sum_{n=0}^{N} \frac{(\xi^2\sigma^2)^n}{2^n n!} \,\mathrm{d}\xi. \tag{28}$$

The right-hand side of equation (28) is obviously finite, since the Gaussian belongs to $S(\mathbb{R})$. Thus, $\hat{\phi}_N \in S_M$ for every $M \geqslant 1$ and $N \geqslant 1$.

Next, we have that (see figures 18 and 19)

$$\begin{aligned} \left|\hat{\phi}_{N,\sigma}(\xi)\right| &= \left| \mathrm{e}^{-\xi^2\sigma^2/2} \sum_{n=0}^{N} \frac{(\xi^2\sigma^2)^n}{2^n n!} \right| \\ &\leqslant \left| \mathrm{e}^{-\xi^2\sigma^2/2} \sum_{n=0}^{\infty} \frac{(\xi^2\sigma^2)^n}{2^n n!} \right| \\ &= \mathrm{e}^{-\xi^2\sigma^2/2} \mathrm{e}^{\xi^2\sigma^2/2} = 1, \end{aligned} \tag{29}$$

and finally we have that (see figure 18)

$$\begin{aligned} \lim_{N\to\infty} \hat{\phi}_{N,\sigma}(\xi) &= \lim_{N\to\infty} \mathrm{e}^{-\xi^2\sigma^2/2} \sum_{n=0}^{N} \frac{(\xi^2\sigma^2)^n}{2^n n!} \\ &= \mathrm{e}^{-\xi^2\sigma^2/2} \lim_{N\to\infty} \sum_{n=0}^{N} \frac{(\xi^2\sigma^2)^n}{2^n n!} \\ &= \mathrm{e}^{-\xi^2\sigma^2/2} \mathrm{e}^{\xi^2\sigma^2/2} = 1. \end{aligned} \tag{30}$$

It is apparent from figures 18 and 19 that when $N \to +\infty$, or $\sigma \to 0$, $\hat{\phi}_{N,\sigma} \to 1$.

Therefore (as also shown in the paper of Chandler and Gibson [7]), Hermite DAFs do indeed yield unity approximations. Moreover, for every $N \geqslant 1$, and $M \geqslant 1$, every ϕ_N belongs to $\mathcal{F}_M$. In addition, Hermite DAFs are C^∞, because $\hat{\phi}_N \in S_M$ for every $M \in \mathbb{Z}^+$.

3.2. The Sinc-class of distributed approximating functionals

The following proposition shows that the Sinc-class of DAFs is not a small one. Throughout the rest of the paper we shall denote the Gaussian with variance σ by g_σ, i.e.,

$$g_\sigma(x) := \frac{1}{\sqrt{2\pi}\,\sigma} \mathrm{e}^{-x^2/(2\sigma^2)}. \tag{31}$$

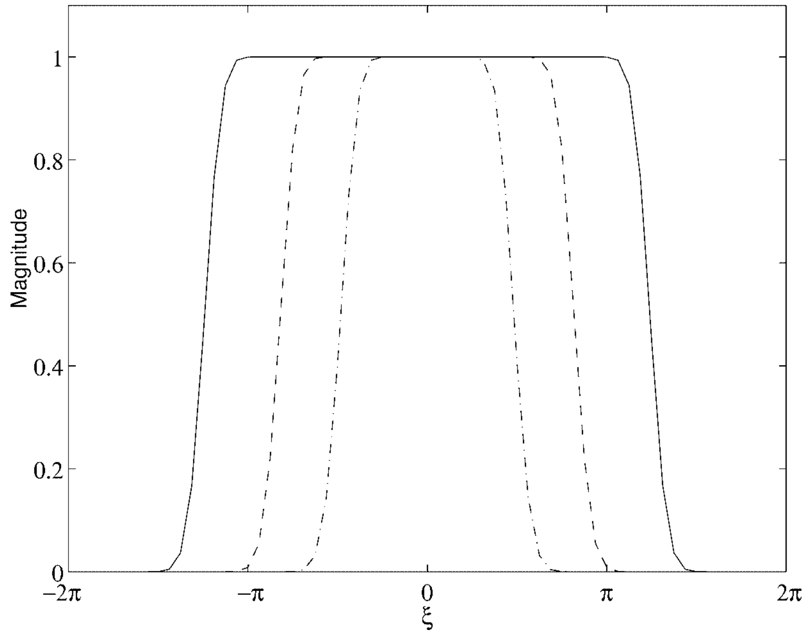

Figure 18. The plot of the Hermite DAF $\phi_{N,3.05}$ in frequency space with the variance σ fixed at 3.05. Dash-dotted line, $N = 10$; dashed line, $N = 30$; and solid line, $N = 70$.

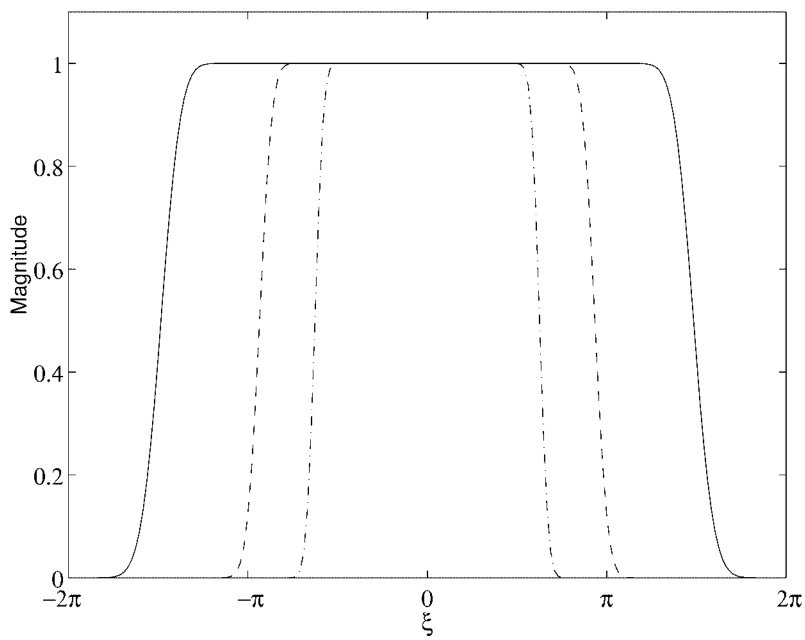

Figure 19. The plot of the Hermite DAF $\phi_{70,\sigma}$ in frequency space with the highest order of the polynomial N fixed at 70. Dash-dotted line, $\sigma = 6.05$; dashed line, $\sigma = 4.05$; and solid line, $\sigma = 2.55$.

Proposition 2. Let $f(x)$ be a function in $\mathbf{L}^2(\mathbb{R})$ satisfying the following properties:

1. The Fourier transform of $f(x)$ is absolutely bounded.
2. $\int_{-\infty}^{+\infty} \hat{f}(\xi)\,\mathrm{d}\xi = \sqrt{2\pi}$.
3. The function $\hat{f}$ is band limited, i.e., there exists $A > 0$ such that $\hat{f}(\xi) = 0$ for every $|\xi| > A$.

Then the sequence $\{\hat{\phi}_n\}_{n=1}^{\infty}$ defined by $\hat{\phi}_n := \hat{f} * \hat{g}_{\sigma_n}$, $n \in \mathbb{N}$, is a unity approximation as $\sigma_n \to 0$.

Proof. The Fourier transform of the Gaussian function g_σ is given by the equation

$$\hat{g}_\sigma(\xi) = \frac{1}{\sqrt{2\pi}} \mathrm{e}^{-\xi^2\sigma^2/2}. \tag{32}$$

Thus, the Fourier transform of the DAF ϕ_n is given by the equation

$$\begin{aligned}\hat{\phi}_n(\xi) &= \big(\hat{f} * \hat{g}_{\sigma_n}\big)(\xi) \\ &= \int_{-\infty}^{+\infty} \hat{f}(\xi - \omega)\hat{g}_{\sigma_n}(\omega)\,\mathrm{d}\omega.\end{aligned} \tag{33}$$

The third property of f implies that

$$\begin{aligned}\hat{\phi}_n(\xi) &= \int_{\xi-A}^{\xi+A} \hat{f}(\xi - \omega)\hat{g}_{\sigma_n}(\omega)\,\mathrm{d}\omega \\ &= \frac{1}{\sqrt{2\pi}} \int_{\xi-A}^{\xi+A} \hat{f}(\xi - \omega)\mathrm{e}^{-\omega^2\sigma_n^2/2}\,\mathrm{d}\omega.\end{aligned} \tag{34}$$

We will prove that $\hat{\phi}_{n,\sigma}$ belongs to S_M for every $M \in \mathbb{Z}^+$:

$$\begin{aligned}&\int_{-\infty}^{+\infty} \big(1 + |\xi| + |\xi|^2 + \cdots + |\xi|^M\big)\big|\hat{\phi}_n(\xi)\big|\,\mathrm{d}\xi \\ &\leqslant \frac{1}{\sqrt{2\pi}} \int_{-\infty}^{+\infty} \big(1 + |\xi| + |\xi|^2 + \cdots + |\xi|^M\big) \\ &\qquad \times \left(\int_{\xi-A}^{\xi+A} \big|\hat{f}(\xi - \omega)\big|\mathrm{e}^{-\omega^2\sigma_n^2/2}\,\mathrm{d}\omega\right)\mathrm{d}\xi.\end{aligned} \tag{35}$$

Now split the right-hand side of the previous inequality into the following three parts:

$$\begin{aligned}
&\int_{-\infty}^{+\infty} \left(1+|\xi|+|\xi|^2+\cdots+|\xi|^M\right)\left(\int_{\xi-A}^{\xi+A} \left|\hat{f}(\xi-\omega)\right|\mathrm{e}^{-\omega^2\sigma_n^2/2}\,\mathrm{d}\omega\right)\mathrm{d}\xi \\
&\quad= \int_{-\infty}^{+A} \left(1+|\xi|+|\xi|^2+\cdots+|\xi|^M\right)\left(\int_{\xi-A}^{\xi+A} \left|\hat{f}(\xi-\omega)\right|\mathrm{e}^{-\omega^2\sigma_n^2/2}\,\mathrm{d}\omega\right)\mathrm{d}\xi \\
&\qquad+ \int_{-A}^{+A} \left(1+|\xi|+|\xi|^2+\cdots+|\xi|^M\right)\left(\int_{\xi-A}^{\xi+A} \left|\hat{f}(\xi-\omega)\right|\mathrm{e}^{-\omega^2\sigma_n^2/2}\,\mathrm{d}\omega\right)\mathrm{d}\xi \\
&\qquad+ \int_{+A}^{+\infty} \left(1+|\xi|+|\xi|^2+\cdots+|\xi|^M\right)\left(\int_{\xi-A}^{\xi+A} \left|\hat{f}(\xi-\omega)\right|\mathrm{e}^{-\omega^2\sigma_n^2/2}\mathrm{d}\omega\right)\mathrm{d}\xi. \qquad (36)
\end{aligned}$$

First, we will consider the first term in this sum.

Assume that $\xi < -A$ and $|\xi-\omega| \leqslant A$. Thus, $\xi - A \leqslant \omega \leqslant \xi + A < 0$. This implies that for every $\omega \in [-A, A]$ we have that

$$\mathrm{e}^{-\omega^2\sigma_n^2/2} \leqslant \mathrm{e}^{-(\xi+A)^2\sigma_n^2/2}. \qquad (37)$$

Therefore,

$$\begin{aligned}
&\int_{-\infty}^{+A} \left(1+|\xi|+|\xi|^2+\cdots+|\xi|^M\right)\left(\int_{\xi-A}^{\xi+A} \left|\hat{f}(\xi-\omega)\right|\mathrm{e}^{-\omega^2\sigma_n^2/2}\,\mathrm{d}\omega\right)\mathrm{d}\xi \\
&\quad\leqslant \int_{-\infty}^{+A} \left(1+|\xi|+|\xi|^2+\cdots+|\xi|^M\right)\left(\int_{\xi-A}^{\xi+A} \left|\hat{f}(\xi-\omega)\right|\mathrm{e}^{-(\xi+A)^2\sigma_n^2/2}\,\mathrm{d}\omega\right)\mathrm{d}\xi \\
&\quad= \int_{-\infty}^{+A} \left(1+|\xi|+|\xi|^2+\cdots+|\xi|^M\right)\mathrm{e}^{-(\xi+A)^2\sigma_n^2/2}\left(\int_{\xi-A}^{\xi+A} \left|\hat{f}(\xi-\omega)\right|\mathrm{d}\omega\right)\mathrm{d}\xi \\
&\quad< \left\|\hat{f}\right\|_1 \int_{-\infty}^{+A} \left(1+|\xi|+|\xi|^2+\cdots+|\xi|^M\right)\mathrm{e}^{-(\xi+A)^2\sigma_n^2/2}\,\mathrm{d}\xi < +\infty, \qquad (38)
\end{aligned}$$

for every finite integer M. Note that since $f \in \mathbf{L}^2(\mathbb{R})$, we have that $\hat{f} \in \mathbf{L}^2(\mathbb{R})$. Since f is band limited, by applying Cauchy–Schwartz inequality we conclude that $\hat{f} \in \mathbf{L}^1(\mathbb{R})$.

An argument similar to the one for the first summand in equation (36) applies for the third summand as well. Obviously, the second term of the right-hand side of equation (36) is finite.

This completes the proof that $\hat{\phi}_n \in S_M$, for every $M \geqslant 1$. This in turn implies that ϕ_n is C^∞.

From equation (34) it becomes apparent that for every $\xi \in \mathbb{R}$ also

$$\left|\hat{\phi}_n(\xi)\right| \leqslant \frac{1}{\sqrt{2\pi}}\left\|\hat{f}_n\right\|_1. \qquad (39)$$

The latter inequality establishes that Sinc-class DAF sequence $\{\phi_n\}$ satisfies the second property.

Finally, we have that for every $\xi \in \mathbb{R}$ and $n \in \mathbb{N}$, the functions $\omega \to \hat{f}(\omega)\mathrm{e}^{-(\xi-\omega)^2\sigma_n^2/2}$ are absolutely integrable and dominated by $|\hat{f}|$. Moreover, $\lim_{n\to\infty} \hat{f}(\omega)\mathrm{e}^{-(\xi-\omega)^2\sigma_n^2 2} = \hat{f}(\omega)$ for every $\omega \in \mathbb{R}$, because $\lim_{n\to\infty} \sigma_n = 0$. Thus, by Lebesgue's dominated convergence theorem we get that

$$\begin{aligned} \lim_{n\to\infty} \hat{\phi}_n(\xi) &= \frac{1}{\sqrt{2\pi}} \int_{-\infty}^{+\infty} \hat{f}(\omega) \lim_{\sigma_n\to 0} \mathrm{e}^{-(\xi-\omega)^2\sigma_n^2/2}\,\mathrm{d}\omega \\ &= \frac{1}{\sqrt{2\pi}} \int_{-\infty}^{+\infty} \hat{f}(\omega)\,\mathrm{d}\omega = 1. \end{aligned} \tag{40}$$

This completes the proof of proposition 2. □

Remark 2. We can generalize the proposition by considering those $f \in \mathbf{L}^2(\mathbb{R})$ satisfying properties 1 and 3 of proposition 2 only and $\int_{-\infty}^{+\infty} \hat{f}(\xi)\,\mathrm{d}\xi = C \neq 0$. Then we can consider the unity approximation $\{\hat{\phi}_n\}_{n\geqslant 1}$, where $\phi_n := (\sqrt{2\pi}/C) f g_{\sigma_n}$.

We shall consider a few examples of Sinc-class DAF sequences of functions that form unity approximations.

Example 2 (2π-periodic Sinc-DAF). If we choose the $\hat{f}$ as the following:

$$\hat{f}(\xi) = \chi_{[-\pi,\pi)}(\xi) = \begin{cases} 1 & \text{for } |\xi| \leqslant \pi, \\ 0 & \text{for } |\xi| > \pi, \end{cases} \tag{41}$$

then the Sinc-DAF is the following:

$$\phi_\sigma(x) = \frac{1}{\sqrt{2\pi}} \mathrm{e}^{-x^2/(2\sigma^2)} \frac{\sin(\pi x)}{\pi x}. \tag{42}$$

More generally, we have the $2a$-periodic Sinc-DAF,

$$\phi_\sigma(x) = \frac{1}{\sqrt{2\pi}} \mathrm{e}^{-x^2/(2\sigma^2)} \frac{\sin(ax)}{ax}. \tag{43}$$

Example 3 (Generalized de la Vallée Poussin DAF). If we take $\hat{f}$ to be given by the following equation:

$$\hat{f}_{\eta,\lambda}(\xi) = \begin{cases} 1 & \text{for } |\xi| \leqslant \eta, \\ \dfrac{|\xi| - \lambda\eta}{\eta(1-\lambda)} & \text{for } \eta \leqslant |\xi| \leqslant \lambda\eta, \\ 0 & \text{otherwise}, \end{cases} \tag{44}$$

where $\eta \geqslant 0$, $\lambda > 1$, then we construct the *Generalized de la Vallée Poussin DAF* based on our preceding remark as

$$\phi_\sigma(x) = \frac{1}{\sqrt{2\pi^3}\sigma} \mathrm{e}^{-x^3/(2\sigma^2)} \frac{\cos(\eta x) - \cos(\lambda\eta x)}{(\lambda - 1)\eta x^2}. \tag{45}$$

Remark 3. Notice that every function of the form fg_σ, where f satisfies properties 1 and 3 of proposition 2, is C^∞, because it belongs to the space $\mathcal{F}_M$ for every positive integer M.

Thus, we have obtained several interesting new DAFs in addition the previous HDAF. Each of these can be used to provide a means of constructing wavelet multiresolution analyses. We expect they will be of interest for a variety of applications in mathematical chemistry.

Acknowledgement

The authors would like to thank the anonymous referee for the valuable suggestions.

References

[1] D.K. Hoffman, N. Nayar, O.A. Sharafeddin and D.J. Kouri, On an analytic banded approximation for the discretized free propagator, J. Phys. Chem. 95 (1991) 8299–8305.
[2] D.K. Hoffman and D.J. Kouri, Distributed approximating function theory for an arbitrary number of particles in a coordinate system-independent formalism, J. Phys. Chem. 97 (1993) 4984–4988.
[3] D.K. Hoffman, A. Frishman and D.J. Kouri, Distributed approximating functional approach to fitting multi-dimensional surfaces, Chem. Phys. Lett. 262 (1996) 393–399.
[4] Z. Shi, D.J. Kouri, G. Wei and D.K. Hoffman, Generalized symmetric interpolating wavelets, Comput. Phys. Commun. 119 (1999) 194–218.
[5] G.W. Wei, S.C. Althorpe, D.J. Kouri and D.K. Hoffman, An application of distributed approximating functional-wavelets to reactive scattering, J. Chem. Phys. 108 (1998) 7065–7069.
[6] G. Wei, D.S. Zhang, S.A. Althorpe, D.J. Kouri and D.K. Hoffman, Wavelet-distributed approximating functional method for solving the Navier–Stokes equation, Comput. Phys. Commun. 115 (1998) 18–24.
[7] C. Chandler and A.G. Gibson, Uniform approximation of functions with discrete approximation functional, J. Approx. Theory 100 (1999) 233–250.
[8] G. Wei, D.J. Kouri and O.K. Hoffman, Wavelets and distributed approximating functionals, Comput. Phys. Commun. 112 (1998) 1–6.
[9] O.K. Hoffman, G. Wei, D. Zhang and D.J. Kouri, Shannon–Gabor wavelet distributed approximating functional, Chem. Phys. Lett. 287 (1998) 119–124.
[10] D.K. Hoffman, G. Wei and D.J. Kouri, A variational approach to the Dirichlet–Gabor wavelet-distributed approximating functional, J. Math. Chem. 25 (1999) 235–244.
[11] W. Rudin, *Principles of Mathematical Analysis* (McGraw-Hill, New York, 1976).
[12] M. Holschneider, *Wavelets, an Analysis Tool* (Oxford University Press, New York, 1995).
[13] E. Hewitt and K. Stronberg, *Real and Abstract Analysis* (Springer-Verlag, 1965).
[14] I. Daubechies, Comm. on Pure Appl. Math., Society of Industrial and Applied Mathematics, Philadelphia (1988).
[15] E. Stein and G. Weiss, *An Introduction to Harmonic Analysis on Euclidean Spaces* (Princeton University Press, 1968).